Exchange interaction of excitons in GaAs heterostructures

E. Blackwood, M. J. Snelling,* and R. T. Harley
Physics Department, Southampton University, Southampton, United Kingdom

S. R. Andrews
School of Physics, University of Bath, Bath, United Kingdom

C. T. B. Foxon
Physics Department, Nottingham University, Nottingham, United Kingdom
(Received 3 June 1994)

The circular polarization of cw photoluminescence as a function of applied magnetic field has been measured at 1.8 K for excitons in a series of GaAs/$Al_xGa_{1-x}As$ and GaAs/AlAs type-I quantum wells having well widths between 2.5 and 8.0 nm. The results show evidence of level crossings, which have been analyzed to give the short-range, spin-dependent exchange interaction. The associated experimental exchange splittings between optically allowed and nonallowed exciton states are of the order of 0.15 meV for the narrowest wells and fall monotonically with increasing width. Simulations of the data using solutions of rate equations for the exciton-level populations show that the optically nonallowed exciton states lie below the allowed states and give insight into the field dependence of the spin-relaxation rates of excitons and of holes and electrons in an exciton. Calculations of the enhancement of exchange interaction due to carrier confinement relative to the bulk value give agreement between the quantum-well and bulk-exchange values, and confirm that exchange is particularly sensitive to barrier height and other details of the structure. The data also show evidence for eigenstate-polarization changes, which indicate a much smaller zero-field splitting due to departure of the quantum-well symmetry from the ideal D_{2d}. The simulation indicates that only a fraction (up to 20%) of excitons in these samples actually experiences a nonideal, distorted environment.

I. INTRODUCTION

The exchange interaction for excitons in GaAs heterostructures has received considerable theoretical attention, both from the fundamental point of view[1-3] and because of the influence it may have on spin relaxation of excitons.[4] It is composed of short-range (so-called analytical) and long-range (nonanalytical) parts. The short-range part gives splittings of the exciton states at $k=0$ corresponding to different orientations of the spins of the particles. The long-range part produces the longitudinal-transverse splitting of the optically allowed exciton states. In three dimensions (3D) the nonretarded longitudinal-transverse splitting is finite as k approaches zero. For a quantum well, however, dimensional arguments show that the splitting must vanish linearly as k becomes small, and is very small for $k \ll L_z^{-1}$, where L_z is the quantum-well width.[2] The interaction is expected to be a sensitive function of the electron-hole overlap and so to vary strongly with well width and with other factors such as barrier height. In simple type-I quantum wells it should be enhanced compared with the value in bulk material, whereas in type-II systems it may be reduced since electrons and holes are confined in spatially separated parts of the structure.[5]

In this paper we are concerned with the short-range exchange interaction in a variety of structures and the associated splitting of the $n=1$ $1s$ heavy-hole–electron exciton into optically allowed $J=1$ and nonallowed $J=2$ components. Good experimental values already exist for type-II GaAs/AlAs quantum wells from optically detected magnetic resonance (ODMR).[6] The exchange splittings increase rapidly as well and barrier widths are reduced and are close to that for bulk GaAs for the narrowest wells and barriers investigated.[7] In type-I quantum wells, however, the exciton lifetimes are too short for ODMR,[8] so that other techniques must be used. We report here measurements of the circular polarization of photoluminescence at 1.8 K in applied magnetic fields in a series of type-I GaAs/$Al_xGa_{1-x}As$ and GaAs/AlAs quantum-well samples.[9] This reveals level crossing (or anticrossing) effects[6,10] and enables the exchange energy of the exciton to be obtained as a function of well width L_z. For this we rely on our previous investigations of magnetic g factors of electrons,[11] heavy holes, and excitons[12] in similar samples. Our interpretation of the level crossing signals is confirmed by model calculations based on solution of the rate equations for transitions between the excitonic levels and radiative decay. The choice of parameters required in these calculations to simulate the measurements strongly suggests that the $J=1$ states are higher in energy than the $J=2$ (in our notation a positive sign for the exchange parameter), and also gives insight into the relative strengths of spin-relaxation processes within the exciton and their magnetic-field dependence.

0163-1829/94/50(19)/14246(9)/$06.00 ©1994 The American Physical Society

There is also evidence for removal of the degeneracy of the $J=1$ component for about 10–20 % of excitons in the inhomogeneous distribution in these samples, similar to that observed in type-II quantum wells,[6] and consistent with reduction of the symmetry below the ideal D_{2d}, for example, near growth steps in the interfaces.

Our experimental values of exchange are much lower than those previously deduced from splittings of the heavy-hole luminescence line in $GaAs/Al_xGa_{1-x}As$ multiple-quantum-well samples.[13] The interpretation of those splittings as due to exchange is questionable[2] since they are incompatible with the measured bulk exchange interaction and the calculated enhancement factors in type-I quantum wells. It seems likely that they were actually caused by well-width fluctuations in the samples.

We have made calculations of the electron-hole overlap, and hence the enhancement factor for the exchange relative to the bulk value, for a variety of structures. The enhancement for type-I $GaAs/Al_xGa_{1-x}As$ and GaAs/AlAs quantum wells combined with the measured short-range exchange splitting in bulk GaAs (20 ± 10 μeV) (Ref. 7) are in satisfactory agreement with the measurements. Since exchange may influence the spin-lattice relaxation of excitons,[4] we have also calculated the enhancement factors for $In_xGa_{1-x}As/GaAs$ strained-layer quantum wells and for a "stepped barrier" quantum-well structure for which spin-lattice relaxation data exist.[14]

II. EXPERIMENTAL METHOD AND MEASUREMENTS

Two series of samples[9] were investigated. Each contained 60 GaAs quantum wells separated by 13.6-nm-wide barriers grown at Philips Research Laboratories by molecular-beam epitaxy (MBE) on a semi-insulating (001)-oriented GaAs substrate. One series had $Al_xGa_{1-x}As$ barriers with Al fraction 0.36 and the second had AlAs barriers. The wells and barriers were not intentionally doped and had low background p-type doping of order 10^{14} cm^{-3}. They were mounted in superfluid liquid helium at about 2 K and magnetic fields were applied along the growth axis with a superconducting magnet. They were illuminated along the growth axis with about 1 W cm^{-2} of linearly polarized light from a dye or Ti-sapphire laser and the $n=1$ heavy-hole exciton luminescence line was detected in a backward direction with $f/10$ optics through a 0.5-m monochromator with photon-counting detection.

Two types of measurements, A and B, were made. In the A measurements (Figs. 1 and 2) the laser was tuned to an energy some tens of meV above the $n=1$ continuum edge and the degree of circular polarization of the wavelength-integrated luminescence was measured as a function of applied field. The circular polarization

$$P\equiv\frac{I_{\sigma^+}-I_{\sigma^-}}{I_{\sigma^+}+I_{\sigma^-}} \tag{1}$$

was obtained using a 50-kHz photoelastic modulator and linear polarizer in front of the monochromator slit in conjunction with a two-channel photon counter gated in synchrony with the modulator. There is a general monotonic increase of $|P|$ with applied field, the sign depending on the direction of the field, with a superimposed peak at a field which varies with quantum-well width. To obtain the positions of the peaks we have subtracted from the raw data an empirically fitted second-order polynomial background; an example of this is shown in Fig. 1(c). The circular polarization of the background and of the peaks was found to be independent of the orientation of the linear polarization of the incident laser and of its photon energy provided that the latter remained within the continuum. We also made subsidiary measurements[15] in which the polarization was measured at different energies within the inhomogeneous luminescence-line profile. This showed that the relative strength of the background and of the peaks changed with the detection energy, the background being relatively more prominent for detection on the low-energy side. Furthermore, when the excitation photon energy was lowered below the continuum,

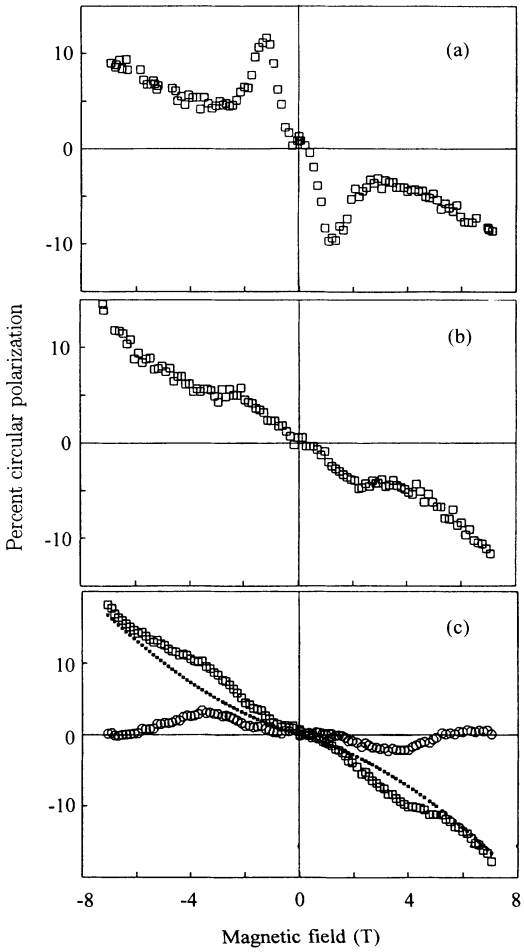

FIG. 1. Circular polarization of integrated luminescence with excitation in the continuum (type-A measurements) for $GaAs/Al_xGa_{1-x}As$ samples with well width (a) 2.57 nm, (b) 5.6 nm, and (c) 7.3 nm. In (c) an empirical background (dotted) is subtracted from the raw data, as described in the text, to allow accurate location of peaks.

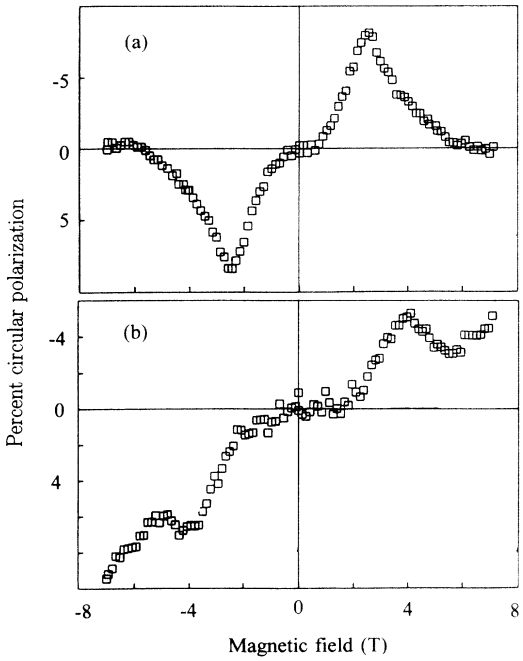

FIG. 2. *A*-type measurements on GaAs/AlAs samples of well width (a) 4.96 nm and (b) 6.51 nm.

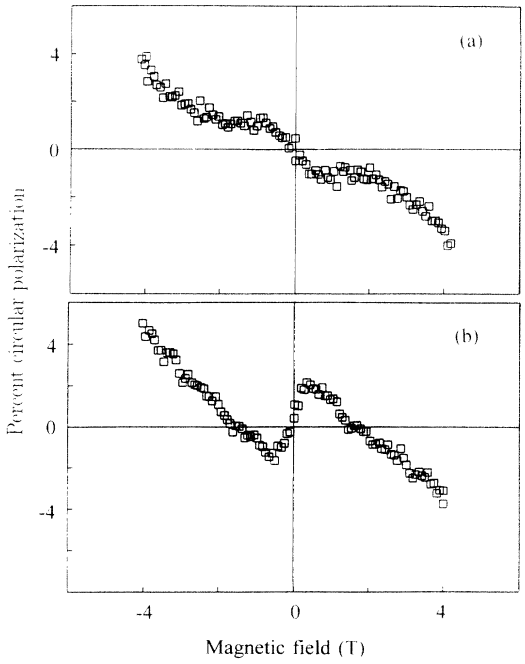

FIG. 4. *B*-type measurements for (a) 7.34-nm well-width GaAs/$Al_xGa_{1-x}As$ sample and (b) 6.51-nm well-width GaAs/AlAs sample.

the peaks appearing in Figs. 1 and 2 became much less prominent or disappeared completely, being replaced by new peaks at lower field which were the subject of the second type of measurement.

In the second type of measurement, *B* (Figs. 3 and 4), the laser was tuned to the heavy-hole exciton absorption peak and the degree of circular polarization P was measured at the peak of the Stokes-shifted luminescence line. Again there is a monotonic increase of $|P|$ with a superimposed anomaly in the form of a dip or a peak; the position of the anomaly varies with well width and in each sample is lower than that observed in the type-*A* measurements. As before, in subsidiary measurements,[15] the relative magnitude of the peaks and the background was found to vary with the detection energy, the background being more prominent at low energies in the luminescence profile. In contrast to the type-*A* measurements, the polarization of the peaks in the *B* case depended strongly on the orientation of the plane of polarization of the exciting beam. The behavior is illustrated in Fig. 5; the "phase" of the peaks relative to the background is re-

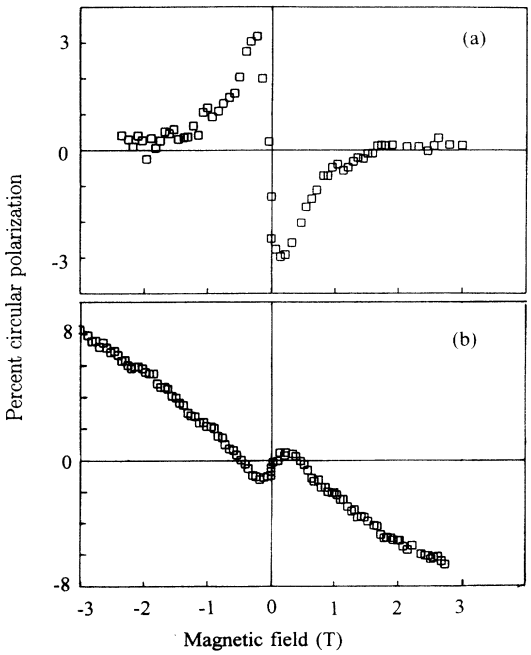

FIG. 3. Circular polarization at peak of luminescence line for linearly polarized excitation parallel to (110) at absorption peak (type-*B* measurements) for GaAs/$Al_xGa_{1-x}As$ samples of well width (a) 2.57 nm and (b) 5.6 nm.

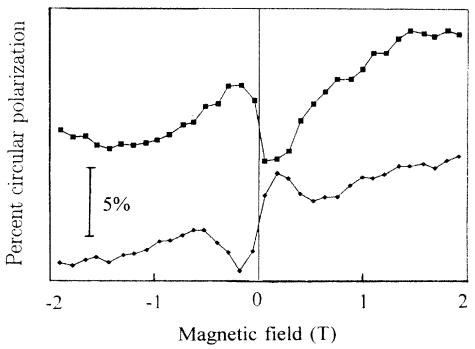

FIG. 5. *B*-type measurement on 2.57-nm well-width GaAs/$Al_xGa_{1-x}As$ sample for excitation linearly polarized along orthogonal (110)-type axes. The zeros of the curves have been arbitrarily shifted.

versed when the exciting polarization is rotated from the (110) to the $(1\bar{1}0)$ crystal axis [growth axis is (001)] and the peaks disappear altogether for polarization along (100) or (010).

III. INTERPRETATION

We interpret the type-A measurements (excitation above the continuum edge) to yield the exchange splitting at zero field between the optically allowed and forbidden exciton states. The type-B series indicate that for a fraction of the excitons the two optically allowed states transform as (110) and $(1\bar{1}0)$ vectors, respectively, and are nondegenerate in zero field. This indicates distortion from the ideal D_{2d} symmetry, with principal basal-plane axes (110) and $(1\bar{1}0)$.

A. Exciton energy levels

The Hamiltonian representing the interaction of a 1s exciton with a magnetic field B can be written as the sum of three terms,

$$H_{\rm ex}=H_e+H_h+H_{eh} \ , \tag{2}$$

representing, respectively, the Zeeman interactions for the electron and the hole and the short-range spin-dependent exchange interaction. We are interested here in the $n=1$ heavy-hole exciton levels in a quantum well grown on a (001) substrate. The Zeeman and exchange splittings are small compared to the heavy- to light-hole splitting and, in our temperature range, the population of the light-hole states is negligible. It is therefore possible, following Ref. 6, to use an effective spin Hamiltonian of the form

$$H_{\rm ex}=\sum_{i=x,y,z}[\mu_B(g_{e,i}S_i-g_{h,i}\Sigma_i)B_i-2c_iS_i\Sigma_i] \ , \tag{3}$$

where $S=\frac{1}{2}$ is the electron spin operator and $\Sigma=\frac{1}{2}$ is an effective spin operator representing the two heavy-hole states $J=\pm\frac{3}{2}$. The parameters g_e and g_h, which are the electron and effective heavy-hole magnetic g factors, and c, which represents the short-range electron-hole exchange interaction, are functions of the quantum-well width.[11,12,6]

The energies of the four heavy-hole exciton states for applied field parallel to z are

$$\begin{aligned}
E_1&=\frac{c_z}{2}-\frac{1}{2}\sqrt{\mu_B^2B_z^2(g_{h,z}+g_{e,z})^2+(c_x+c_y)^2} \ ,\\
E_2&=\frac{c_z}{2}+\frac{1}{2}\sqrt{\mu_B^2B_z^2(g_{h,z}+g_{e,z})^2+(c_x+c_y)^2} \ ,\\
E_3&=-\frac{c_z}{2}+\frac{1}{2}\sqrt{\mu_B^2B_z^2(g_{h,z}-g_{e,z})^2+(c_x-c_y)^2} \ ,\\
E_4&=-\frac{c_z}{2}-\frac{1}{2}\sqrt{\mu_B^2B_z^2(g_{h,z}-g_{e,z})^2+(c_x-c_y)^2} \ .
\end{aligned} \tag{4}$$

The levels are plotted in Fig. 6 for field parallel to z for the ideal D_{2d} symmetry and for $c_x,c_y \ll c_z$ (see below for justification of this assumption). The z component of exchange causes a zero-field splitting between the optically allowed and nonallowed states and the x and y components cause small additional zero-field splittings. D_{2d} has a fourfold rotation-reflection axis along the growth direction (z) which dictates $c_x=-c_y$ as well as $g_{e,x}=g_{e,y}$, $g_{h,x}=-g_{h,y}$,[6] so that E_1 and E_2 are degenerate in zero field. If this symmetry is broken a zero-field splitting c_x+c_y appears. Optical transitions to E_1 and E_2 are electric-dipole allowed whereas E_3 and E_4 are forbidden.

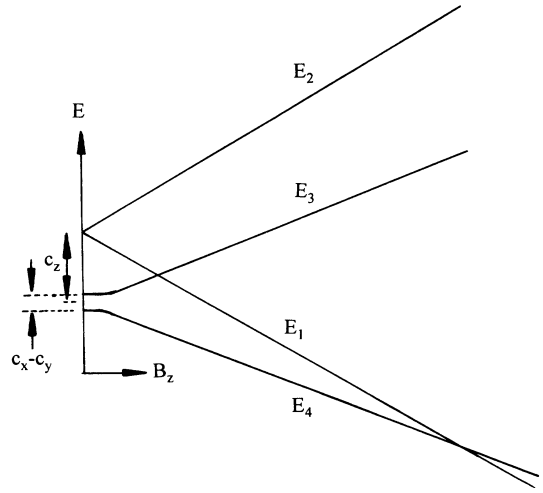

FIG. 6. Exciton energy levels given by Eq. (4) for $c_x=-c_y$ (ideal D_{2d} symmetry). E_1 and E_2 are optically allowed with σ^+ and σ^- polarizations.

Independent of the actual symmetry we expect[11] on the basis of $\mathbf{k}\cdot\mathbf{p}$ theory that g_e will be nearly isotropic ($g_{e,x}\approx g_{e,y}\approx g_{e,z}$). In contrast, the effective hole g factor is related to the valence-band parameters κ and q which appear in the Luttinger Hamiltonian and which are coefficients, respectively, of the linear Zeeman term J_iB_i and of the higher-order term $J_i^3B_i$, where J_i are the true valence-band angular-momentum operators. This leads to[6]

$$g_{h,x}=3q_x, \quad g_{h,y}=-3q_y, \quad g_{h,z}=6\kappa_z+13.5q_z \ , \tag{5}$$

and, since in general $q \ll \kappa$, we expect that $g_{h,x}$ and $g_{h,y}$ will be small compared to $g_{h,z}$. Similarly c_x and c_y will be small since they are coefficients of spin-spin terms of the form $J_i^3S_i$ whereas the leading contribution to c_z comes from the linear term J_zS_z. We do not have direct experimental evidence for the relative magnitudes of these coefficients in type-I GaAs quantum wells but ODMR studies of type-II systems[6] have confirmed that $g_{h,z} \gg g_{h,x},g_{h,y}$ and also that $c_z \gg c_x,c_y$.

B. Qualitative interpretation of experiments

We have previously obtained values of the g factors as functions of quantum-well width for type-I GaAs quantum wells from measurements of the Hanle effect[11] and Zeeman spectroscopy.[12] These have shown that the magnetic splittings of the exciton are very small compared to the inhomogeneous broadening due to well-width fluctua-

tions. Consequently, the total luminescence intensity measured with the spectral resolution used here is proportional to the combined photoexcited population of the dipole-allowed exciton levels. Similarly, the net polarization of the luminescence is given by the sum of populations of each level weighted by the polarization corresponding to the appropriate eigenvector.

In the effective spin notation $|\Sigma_z,S_z\rangle$ the four basis states are

$$\begin{aligned}\phi_a &= |-\tfrac{1}{2},+\tfrac{1}{2}\rangle \quad (\sigma^-)\,,\\ \phi_b &= |+\tfrac{1}{2},-\tfrac{1}{2}\rangle \quad (\sigma^+)\,,\\ \phi_c &= |-\tfrac{1}{2},-\tfrac{1}{2}\rangle,\quad \phi_d = |+\tfrac{1}{2},+\tfrac{1}{2}\rangle\,,\end{aligned} \tag{6}$$

where ϕ_a and ϕ_b are optically allowed, transforming as σ^- and σ^+ polarizations, and ϕ_c and ϕ_d are forbidden. In the ideal D_{2d} symmetry ϕ_a and ϕ_b are eigenstates for all values of field giving purely circularly polarized transitions. For lower symmetry, these states become approximate eigenstates of the Hamiltonian (2) for applied field such that

$$|(g_{ez}+g_{hz})\mu_B B_z| > |c_x|,|c_y|$$

and the optical transitions then have close-to-circular polarization. However, at lower fields the transverse components of the exchange mix the basis states and at zero field the eigenstates transform as x and y, so that the allowed optical transitions have linear polarization. In the discussion which follows, the polarization anomaly found in the type-B measurements at low fields corresponds to the transition from linear to circular polarized eigenstates and indicates departure from D_{2d} symmetry with x and y corresponding to (110) and $(1\bar{1}0)$. The polarization anomalies in the type-A measurements occur at considerably higher fields and therefore in their interpretation we take the optically active eigenstates to be circularly polarized.

In the type-A measurements the electron-hole pairs are photogenerated in the continuum. These will form heavy-hole excitons in each of the four spin states with equal probability and the relative populations of the states under cw excitation will be determined by the balance of recombination processes and phonon-assisted relaxation between the levels. Thus populations of the two optically allowed levels will tend towards the Boltzmann thermal distribution, with the degree of thermalization depending on the relaxation rates between levels. If these rates vary smoothly the population difference of the optically allowed levels will increase steadily with applied field. However, we expect that the transition rate between a pair of levels will increase sharply if their energies become equal, because the transition can then occur without the intervention of a phonon. This will be reflected in an anomaly in the population difference of the optically allowed levels and therefore in the degree of circular polarization P of the integrated luminescence.

Referring to Fig. 6, there are in general two fields at which levels cross. If we assume c_x and c_y to be small, they are given by

$$\begin{aligned}B_z^{(h)} &\approx \frac{c_z}{g_{h,z}\mu_B}\,,\\ B_z^{(e)} &\approx \frac{c_z}{g_{e,z}\mu_B}\,.\end{aligned} \tag{7}$$

We expect to observe an anomaly in P superimposed on the smooth background increase at each of these fields. However, from our measurements of g factors,[11,12] we know that for the well widths investigated here $|g_{h,z}| \gg |g_{e,z}|$. We therefore associate the single observed peak for each sample with $B_z^{(h)}$, in which case $B_z^{(e)}$ would be beyond the range of measurement. This identification leads to the values of c_z plotted in Fig. 7. The main source of uncertainty in these values is associated with that of $g_{h,z}$.[12] The full curves in Fig. 7 are the results of calculations of the exchange enhancement described in Sec. III D.

In the type-B measurements excitons are generated by resonant optical excitation with linearly polarized light into the two optically allowed states (E_1 and E_2) only. The rate of generation of excitons in each of the two levels will depend on the eigenvector and on the orientation of the polarization. Similarly, the degree of circular polarization of the luminescence will depend on the degree of thermalization due to transitions between the levels and on their eigenvectors. In the case of D_{2d} symmetry the eigenvectors of the states are pure σ^+ and σ^- for all fields, and linearly polarized excitation will give equal level populations for all fields. Therefore if we neglect effects of transitions between the excitation levels the degree of circular polarization P of the luminescence will be zero for all fields. Inclusion of thermalization will lead to a smooth increase of $|P|$ with field. In the case of lower symmetry the eigenvectors are linear in zero field, elliptical for intermediate fields, and become $\sigma^\pm$ at high field.

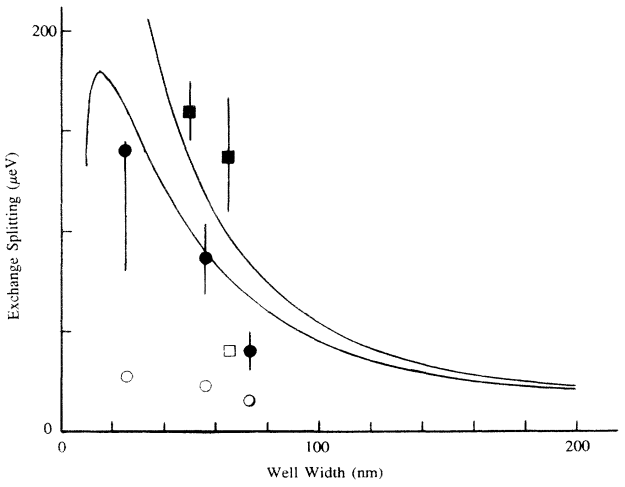

FIG. 7. Zero-field splittings for heavy-hole excitons in GaAs/$Al_xGa_{1-x}As$ (circles) and GaAs/AlAs (squares) quantum wells. Filled symbols are values of short-range exchange splitting (c_z) obtained from A-type measurements and open symbols are splitting due to nonideality of exciton environment (c_x+c_y) from type-B measurements.

The circular polarization of the luminescence P would then be expected to be zero at zero field and, neglecting thermalization, also zero at high field. However, at intermediate field P will in general have a finite value with a peak or a dip occurring at a value of field given by

$$c_x + c_y \approx \mu_B B_z (g_{h,z} + g_{e,z}) \tag{8}$$

(it can be shown using the formalism of Sec. III C that this relationship is exact if thermalization among the levels is neglected). The peak or dip will be greatest when the exciting polarization coincides with the major or minor axis of the ellipse of the eigenfunctions so that excitons are formed as far as possible in just one of the optically allowed levels. For orientation at 45° to this there will be no anomaly. Comparing these expectations with the type-B measurements, we can deduce that for these particular samples the symmetry is lower than D_{2d} and that the major and minor axes of the eigenfunction ellipses coincide with (110) and $(1\bar{1}0)$ axes of the sample. From the fields at which peaks or dips occur in the data we use Eq. (8) and our previously measured g factors[11,12] to obtain the values of zero-field splitting ($|c_x + c_y|$) plotted in Fig. 7. Again the major uncertainty in these values is from the g factors. We shall see that the magnitude of the observed anomalies indicates that a minority of exciton recombination comes from these distorted regions.

C. Rate equation calculations

To test this qualitative interpretation of the measurements we have carried out simulations of the circular polarization P under different conditions of cw excitation. P is given by

$$P = \frac{N_1 - N_2}{N_1 + N_2} \frac{\mu_B B_z (g_{h,z} + g_{e,z})}{E_1 - E_2} , \tag{9}$$

where N_i ($i = 1$ to 4) are the steady-state populations of the exciton energy levels [Eq. (4)] and we assume that the total luminescence intensity is proportional to the combined populations of the optically allowed levels, 1 and 2. The second factor in Eq. (9) allows for the fact that when $(c_x + c_y) \neq 0$ (i.e., when the symmetry is distorted from D_{2d}) the eigenstates 1 and 2 are not purely circularly polarized. This factor has a negligible effect at all but very low values of magnetic field.

The populations are solutions of the equations

$$\begin{bmatrix} -\tau_r^{-1} - W_{12} - W_{13} - W_{14} & W_{21} & W_{31} & W_{41} \\ W_{12} & -\tau_r^{-1} - W_{21} - W_{23} - W_{24} & W_{32} & W_{42} \\ W_{13} & W_{23} & -W_{31} - W_{32} & 0 \\ W_{14} & W_{24} & 0 & -W_{41} - W_{42} \end{bmatrix} \begin{bmatrix} N_1 \\ N_2 \\ N_3 \\ N_4 \end{bmatrix} + \begin{bmatrix} p_1 \\ p_2 \\ p_3 \\ p_4 \end{bmatrix} = 0 , \tag{10}$$

where τ_r^{-1} is the rate for exciton recombination out of levels 1 and 2. The transition rate W_{ij}, from state i to state j, has the form

$$W_{ij} = \frac{\alpha_{ij} |E_j - E_i|^3}{|\exp[(E_j - E_i)/kT] - 1|} + \frac{\beta_{ij} \Gamma_{ij}^2}{(E_j - E_i)^2 + \Gamma_{ij}^2} , \tag{11}$$

where $\alpha_{ij} = \alpha_{ji}$ and $\beta_{ij} = \beta_{ji}$ are adjustable parameters representing the strengths of different relaxation processes, and $\Gamma_{ij} = \Gamma_{ji}$ is a width which may be related to the exciton momentum relaxation time τ_p by $\Gamma \sim \hbar/\tau_p$.[4] The first term is the standard form for direct-process spin-lattice relaxation involving absorption or emission of a phonon,[16] and the second term describes transitions between quasidegenerate states, for example, at level crossing fields or at zero field.[4] Transitions between the optically allowed states (1 and 2) correspond to simultaneous spin flips of electron and hole and may be regarded as exciton spin flips. Transitions between levels 1 and 3 and between 2 and 4 correspond to hole spin flips only, while transitions between 2 and 3 and between 1 and 4 correspond to electron spin flips only. Thus the simulation contains three independent values each of α_{ij} and β_{ij} which correspond to exciton, hole, and electron spin-flip transitions. Maialle, Andrada e Silva, and Sham,[4] show that at zero field the dominant contribution to these mutual electron-hole spin flips is from exchange interaction and also find it to be the dominant relaxation process in analysis of the zero-field data of Bar-Ad and Bar-Joseph.[14] We expect the hole flip rate to be considerably greater than the electron flip rate due to the strong spin-orbit interaction in the valence band. We set the transition rate between the two optically nonallowed states (3 and 4) to zero[4] since the transition cannot occur through the exchange mechanism which dominates the 1-to-2 transitions. For this steady-state calculation the W_{ij} are specified in units of τ_r^{-1}.

The quantities p_i represent the rates of excitation of the levels and have different values to describe the A and B measurements; for A we have

$$p_1 = p_2 = p_3 = p_4 = 1 \tag{12}$$

and for B with linear polarization along a (110)-type axis

$$p_{1,2} = 1 \pm \frac{c_x + c_y}{E_2 - E_1}, \quad p_{3,4} = 0 . \tag{13}$$

Here the second term in $p_{1,2}$ allows for the fact that the states are not purely linearly polarized.

We have not attempted a detailed fit of this theory to the experimental data but instead have investigated the general behavior of P for a range of choices of the parameters. Figure 8 shows illustrative examples of the results for a 2.57-nm GaAs/$Al_xGa_{1-x}As$ multiple-quantum-well sample. These curves should be compared with Figs. 1(a) and 3(a).

The theory will simulate the type-A data in both shape and magnitude provided that the positive value of c_z is always used. This is a strong indication that the optically allowed states are energetically above the nonallowed states in this system. The simulation of experiment A is not sensitive to the values of c_x and c_y provided their magnitudes are less than c_z, which is expected from the discussion in Sec. III A. For a good representation of the A data, it is also necessary to assume an effective temperature of the excitons in the range 5–10 K, considerably above the ambient sample temperature to 1.8 K. This does not seem unreasonable since the electrons and holes are generated in the continuum and thermalization is not complete before recombination occurs. Apart from the variation of g factors and exchange interactions with well width, the main difference between the data for different samples appears to be this effective temperature. In wider wells the effective exciton temperature is nearer to the lattice temperature, leading to a more rapid increase of background polarization with field.

Figure 9 shows the inverse relaxation times between level pairs corresponding to the calculation of Fig. 8. These are given by

$$\tau_{ij}^{-1} = W_{ij} + W_{ji} \ . \tag{14}$$

The sharp maxima in the exciton flip rate τ_{12}^{-1}, and in τ_{13}^{-1} (one of the hole-flip transitions) are associated with the second term in Eq. (11) whereas the increase in all the rates at high fields comes from the first term. We believe that this figure gives an indication, to within a factor of 5, of the true variation of the relaxation times and their relationship to τ_r^{-1}. The values of Γ_{ij} were taken as 0.02 meV which corresponds to $\tau_p = 25$ ps. The anomaly in the A configuration is particularly sensitive to Γ_{13} and disappears completely for a fivefold increase corresponding to $\tau_p = 5$ ps. From Fig. 9 we can see that over much of the field range the recombination rate dominates all others. The optically nonallowed states therefore tend to act as a population reservoir which normally feeds the allowed states via relatively weak transition mechanisms. However, at the crossing of levels 1 and 3 the feeding of level 1 is enhanced relative to that of level 2, giving the anomaly in polarization.

In the simulation of the B-type measurements the position of the polarization anomaly corresponds quite well with the value of B given by Eq. (8), confirming the use of Eq. (8) to obtain experimental values of $(c_x + c_y)$. However, in contrast to the A case, the theory for the B-type experiment, while having the correct general shape, predicts an anomaly which is considerably too large [compare Figs. 8(b) and 3(a)]. The size of the anomaly in the simulation may be reduced by reducing the exciton spin-

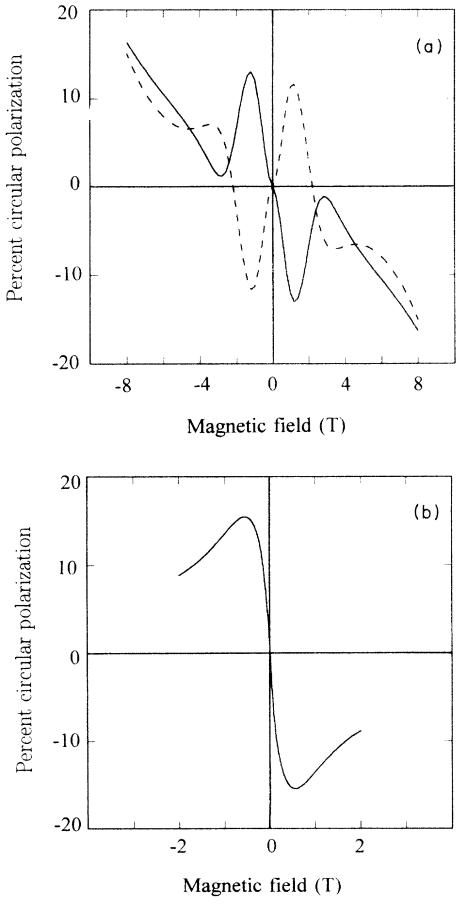

FIG. 8. Simulated polarization for 2.57-nm well-width GaAs/$Al_xGa_{1-x}As$ sample using experimental splittings plotted in Fig. 7 for (a) A-type experiment and (b) B-type experiment. The dashed line is the result for negative c_z. The effective temperature is set at 7 K and the values of transition rates are indicated in Fig. 9 below.

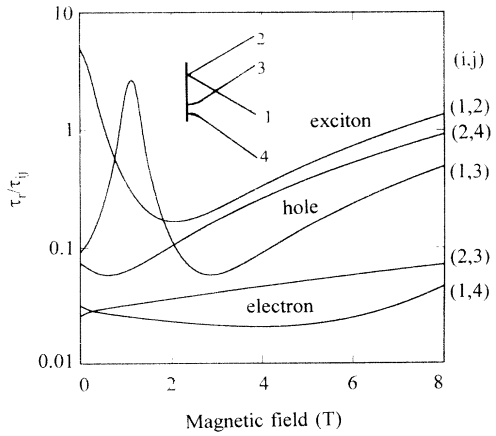

FIG. 9. Field dependence of relaxation times τ_{ij} defined in Eqs. (11) and (14) corresponding to the simulation of Fig. 8. Inset indicates the energy levels [Eq. (4)] and their labels.

flip time τ_{12} but its shape does not then agree with the experiment, suggesting that this is not the origin of the discrepancy. Instead we suggest that the small anomaly in the *B*-type measurements indicates that only a fraction, about 10–20 %, of the luminescence is due to decay of excitons in an environment of lower than the ideal D_{2d} symmetry and the remainder are in ideal environments so do not contribute.

D. Calculation of exchange enhancement

We have calculated the enhancement of the exchange interaction F_{ex} in type-I GaAs/$Al_{0.3}Ga_{0.7}As$, GaAs/AlAs, and $In_{0.11}Ga_{0.89}As$/GaAs quantum wells compared to bulk well material from the changes of electron-hole overlap in quantum-confined excitons. The results are shown in Fig. 10. The z components of the electron and hole wave functions [$\psi_e(z_e)$ and $\psi_h(z_h)$, respectively] were first obtained from solution of the separated Schrödinger equation under appropriate boundary conditions. In the case of $In_xGa_{1-x}As$ account was taken of the effect of lattice strain on the valence-band structure following the treatment of Huang *et al.*[17] These wave functions were then used in a variational calculation in which the exciton wave function was described by

$$\Psi_{ex}(\mathbf{r}) = a(\lambda,\delta)\Psi_e(z_e)\Psi_h(z_h)\exp(-\lambda^{-1}\sqrt{x^2+y^2+\delta^2 z^2}) = \Psi_e(z_e)\Psi_h(z_h)\phi(x,y,z) , \quad (15)$$

where x, y, and z are relative coordinates of the electron and hole and $a(\lambda,\delta)$ is the normalization constant. In this method there are two variational parameters (λ and δ) which are varied to minimize the exciton energy. The effective dielectric constant and in-plane masses were described by weighted averages of the well and barrier values with weights proportional to the probability of the carriers being in well or barrier. The wave function Eq. (15) gives the correct limiting behavior of exciton binding energy and of exchange enhancement as the well width becomes very small or very large. The exchange enhancement is taken as

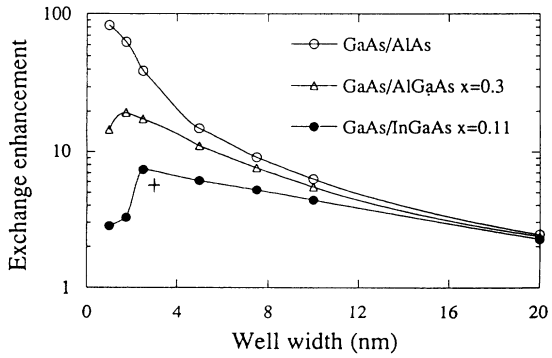

FIG. 10. Calculated enhancement of exchange interaction for 1*s* $n=1$ heavy-hole excitons in various heterostructures. Points and lines are for regular type-I excitons and the cross is for an exciton in a "stepped-barrier" quantum well, as described in the text.

$$F_{exp} = \frac{|\phi_{QW}(0)|^2}{|\phi_{bulk}(0)|^2}\int_{-\infty}^{\infty}|\Psi_e(z_e)\Psi_h(z_h)|^2 dz . \quad (16)$$

In calculating F_{ex} we have used a conduction- to valence-band offset ratio of 0.6 and a chosen set of bulk and quantum-well z-axis effective masses.[18] The xy-plane hole masses were calculated from these using the Kohn-Luttinger formalism.

The additional enhancement for AlAs compared to $Al_xGa_{1-x}As$ barriers (see Fig. 10) is due primarily to the increased confinement resulting from greater barrier height. The calculations for $In_xGa_{1-x}As$ wells show a very much smaller enhancement than for GaAs wells. This is due to the fact that the barriers in this system are much lower, giving less effective carrier confinement. The exchange enhancement in all three cases tends to saturate for narrow wells because as the confinement energy increases towards the barrier height the wave functions tend to spread into the barriers. The effect is particularly marked for $In_xGa_{1-x}As$, the heavy-hole valence-band well in this case being particularly shallow. A similar saturation occurs for the exciton binding energy.

The calculations for GaAs quantum wells from Fig. 10, are superposed on the experimental data in Fig. 7. The theoretical curves give a satisfactory representation of the measurements. They have been normalized to $c_z = 6$ μeV at infinite well thickness which agrees with the measured exchange interaction in bulk GaAs [10±5 μeV (Ref. 7)].

The exchange enhancement for a 3-nm GaAs quantum well bounded by 10-nm layers of $Al_{0.1}Ga_{0.9}As$ which are in turn bounded by thick $Al_{0.3}Ga_{0.7}As$ barriers, as used in the spin-relaxation measurements of Bar-Ad and Bar-Joseph,[14] is calculated using the same method to be 5.6 relative to bulk GaAs and is plotted in Fig. 10 as a single cross. This enhancement is about a factor of 3 less than for regular $Al_xGa_{1-x}As$ barriers due to the much weaker confinement of carriers by the stepped barriers.

IV. SUMMARY AND CONCLUSIONS

We have used measurements of the degree of circular polarization vs magnetic field of photoexcited luminescence in a series of type-I GaAs quantum wells to obtain values of the short-range electron-hole exchange interaction (type-*A* measurements) and to demonstrate the existence of distortions from the ideal D_{2d} symmetry of the wells (type-*B* measurements). The precision of the results is limited by our knowledge of the electron and hole g factors in these systems, which have been obtained in earlier studies.[11,12] Nonetheless, the exchange interaction increases rapidly as the well width decreases and as the barrier height increases. The values are in satisfactory agreement with calculations of the enhancement of the exchange relative to the bulk value due to enhanced electron-hole overlap. This resolves a long-standing controversy caused by the fact that previous experimental values of exchange,[13] obtained by a less reliable method, were too large to be compatible with the bulk value and the calculated enhancement factors.[2,7,13]

Simulations of the *A*-type data, based on steady-state solutions of the rate equations for relaxation among the

exciton levels and recombination, indicate that at zero magnetic field the exciton spin flip is the dominant relaxation rate but that this falls rapidly as the field is increased. For fields above a fraction of a tesla the hole spin-flip transitions become of comparable strength. Simulation of the B measurements suggests that a distorted environment is experienced by about 10–20 % of excitons, the majority being in the ideal D_{2d} environment. These distortions have (110) and $(1\bar{1}0)$ as principal axes and are likely to be associated with growth steps in the interfaces.

We have carried out calculations of the exchange enhancement for two systems which we have not studied experimentally, namely, strained-layer $In_xGa_{1-x}As/GaAs$ quantum wells and a stepped-barrier $GaAs/Al_xGa_{1-x}As$ quantum-well structure.[14] These show, as would be expected, that the enhancement is a strong function of the degree of quantum confinement. These calculations are interesting because the exchange interaction is important for spin relaxation of excitons at zero magnetic field.

ACKNOWLEDGMENTS

This work has been supported by the Science and Engineering Research Council.

*Present address: Clarendon Laboratory, Parks Road, Oxford, U.K.

[1]L. C. Andreani, F. Bassani, and A. Quattropani, Nuovo Cimento D **10**, 1473 (1988).

[2]L. C. Andreani and F. Bassani, Phys. Rev. B **41**, 7536 (1990).

[3]U. Rossler, S. Jorda, and D. Broido, Solid State Commun. **73**, 209 (1990).

[4]M. Z. Maialle, E. A. de Andrada e Silva, and L. J. Sham, Phys. Rev. B **47**, 15 776 (1993).

[5]B. Rejaei Salmassi and G. E. W. Bauer, Phys. Rev. B **39**, 1970 (1989).

[6]H. W. van Kesteren, E. C. Cosman, W. A. J. A. van der Poel, and C. T. Foxon, Phys. Rev. B **41**, 5283 (1990).

[7]W. Ekardt, K. Lösch, and D. Bimberg, Phys. Rev. B **20**, 3303 (1979).

[8]A. S. Plaut, D.Phil. thesis, Oxford University, 1988.

[9]J. W. Orton, P. F. Fewster, J. P. Gowers, P. Dawson, K. J. Moore, P. J. Dobson, C. J. Curling, C. T. Foxon, K. Woodbridge, G. Duggan, and H. I. Ralph, Semicond. Sci. Technol. **2**, 597 (1987).

[10]J. M. Trombetta, T. A. Kennedy, W. Tseng, and D. Gammon, Phys. Rev. B **43**, 2458 (1991).

[11]M. J. Snelling, G. P. Flinn, A. S. Plaut, R. T. Harley, A. C. Tropper, R. Eccleston, and C. C. Phillips, Phys. Rev. B **44**, 11 345 (1991).

[12]M. J. Snelling, E. Blackwood, C. J. McDonagh, R. T. Harley, and C. T. B. Foxon, Phys. Rev. B **45**, 3922 (1992).

[13]R. Bauer, D. Bimberg, J. Christen, D. Oertel, D. Mars, J. N. Miller, T. Fukunaga, and H. Nakashima, in *Proceedings of the Eighteenth International Conference on the Physics of Semiconductors, Stockholm, 1986,* edited by O. Engstrom (World Scientific, Singapore, 1987), p. 525. See also Y. Chen, B. Gil, P. Lefebvre, and H. Mathieu, Phys. Rev. B **37**, 6429 (1988); M. Potemski, J. C. Maan, A. Fasolino, K. Ploog, and G. Weimann, Surf. Sci. **229**, 151 (1990).

[14]S. Bar-Ad and I. Bar-Joseph, Phys. Rev. Lett. **68**, 349 (1992).

[15]E. Blackwood, Ph.D. thesis, Southampton University, 1993; M. J. Snelling, Ph.D. thesis, Southampton University, 1991.

[16]See, for example, R. Orbach, Proc. R. Soc. London Ser. A **264**, 458 (1961).

[17]G. Ji. D. Huang, U. K. Reddy, T. J. Henderson, P. Houdre, and H. Morkoc, J. Appl. Phys. **62**, 3366 (1987).

[18]Bulk effective masses for $Al_yGa_{1-y}As$: $m_e^*=0.067+0.083y$ and $m_{hh}^*=0.45+0.31y$. Quantum-well effective masses for $Al_yGa_{1-y}As$: $m_e^*=0.067+0.083y$, $m_{lh,z}^*=0.094+0.056y$, and $m_{hh,z}^*=0.34+0.42y$. Quantum-well effective masses for $In_yGa_{1-y}As$: $m_e^*=0.029-0.06y$, $m_{lh,z}^*=0.094-0.014y$, and $m_{hh,z}^*=0.34+0.01y$.